Electronic Supplementary Information

Experimental Section

Materials: NH_4F and urea were bought from Beijing Chemical Works. $Ni(NO_3)_2 \cdot 6H_2O$ and $H_2PtCl_6 \cdot 6H_2O$ were purchased from Aladdin Ltd. (Shanghai, China). Pt/C (20 wt% Pt) was provided by Alfa Aesar (China) Chem. Co. Ltd. Nafion (5 wt%) was bought from Sigma-Aldrich Chemical Reagent Co., Ltd. All reagents were used as received without further purification. Ti mesh was purchased from Phychemi Hong Kong Company Limited. Pure water was utilized to prepare all solutions.

Preparation of $Ni(OH)_2$ NS/Ti: We chose Ti mesh as the substrate due to its excellent chemical and electrochemical stability, acceptable electronic conductivity, open structure and ease of fabrication into electrodes.[1] Ti mesh was cleaned by sonication sequentially in concentrated HCl, ethanol and water for several times to remove the surface impurities. $Ni(OH)_2$ NS/Ti was made as follows. In brief, 1.308 g $Ni(NO_3)_2 \cdot 6H_2O$, 1.201 g urea, and 0.296 g NH_4F were dissolved in 80 mL ultrapure water. Then the mixture solution and the pre-treated Ti mesh (2 cm × 3 cm) were transferred into a 100 mL Teflon-lined stainless-steel autoclave and maintained at 373 K for 6 h. After the autoclave cooled down naturally, the resulting $Ni(OH)_2$ NS/Ti was taken out and washed with ultrapure water. The loading of $Ni(OH)_2$ on Ti mesh is 1.49 mg cm^{-2}.

Preparation of $Ni(OH)_2$-PtO_2 NS/Ti: $Ni(OH)_2$-PtO_2 NS/Ti was prepared as follows. $H_2PtCl_6 \cdot 6H_2O$ (2 mg) was dissolved in 25 mL water under vigorous stirring for 5 min. $Ni(OH)_2$ NS/Ti and $H_2PtCl_6 \cdot 6H_2O$ aqueous solution were all transferred into a 50 mL Teflon-lined stainless autoclave and maintained at 373 K for 4 h. After cooled down to room the temperature, the $Ni(OH)_2$-PtO_2 NS/Ti was taken out and washed with ultrapure water thoroughly before vacuum dried. The loading of $Ni(OH)_2$-PtO_2 on Ti mesh is 1.48 mg cm^{-2}.

Preparation of PtO_2/Ti: $H_2PtCl_6 \cdot 6H_2O$ (70 mmol) was dissolved in ultrapure water (30 mL). Then this pale yellow solution was transferred into a 50 mL Teflon-lined stainless-steel autoclave, which was sealed and maintained at 453 K for 24 h. After the sample cooled down to ambient temperature, PtO_2 was collected by centrifugation and washed with ultrapure water. To prepare PtO_2 loaded electrode, 20 mg PtO_2 and 10 μL 5 wt% Nafion solution were dispersed in 1 mL 1:1 v water/ethanol solvent by 30-min sonication to form an ink finally. Then 74 μL catalyst ink was loaded on Ti mesh with a catalyst loading of 1.48 mg cm^{-2}.

Characterizations: XRD data was performed using a LabX XRD-6100 X-ray diffractometer Cu Kα radiation (40 kV, 30 mA) of wavelength 0.154 nm (SHIMADZU, Japan). SEM images were collected from the tungsten lamp-equipped SU3500 scanning electron microscope at an accelerating voltage of 20 kV (HITACHI, Japan). TEM images were collected on a Zeiss Libra 200FE transmission electron microscope operated at 200 kV. XPS measurements were performed using an ESCALABMK II X-ray photoelectron spectrometer with the exciting source of Mg. The ICP-MS analysis was performed on ThermoScientific iCAP6300.

Electrochemical measurements: All electrochemical measurements were performed with a CHI 660E electrochemical analyzer (Chenhua, Shanghai) in a conventional three electrode system, using $Ni(OH)_2$-PtO_2 NS/Ti as working electrode, a graphite rod as counter electrode and Hg/HgO as reference electrode. Polarization curves were obtained using LSV with a scan rate of 5 mV s^{-1} and no activation was used before recording the polarization curves. Given that as-measured reaction currents do not directly reflect the intrinsic behavior of catalysts due to the effect of ohmic resistance, an *iR* correction was applied to all LSV curves for further analysis, and all potentials were reported on a reversible hydrogen electrode (RHE) scale unless specifically stated. The potentials were calibrated to RHE, using the following equation: E (RHE) = E (Hg/HgO) + (0.098 + 0.059 pH) V.

Calculation details: Spin-polarized density functional theory calculations were performed using the Vienna ab initio simulation package (VASP).[2-4] We used the PBE functional for the exchange-correlation energy[5] and projector augmented wave (PAW)

potentials.[6,7] The kinetic energy cutoff was set to 450 eV. The ionic relaxation was performed until the force on each atom is less than 0.02 eV/Å. The k-points meshes were 6 × 6 × 1 with Monkhorst-Pack method.[8] The simulations were performed based on a PtO_2(111) slab model, a $Ni(OH)_2$(001) slab model and $Ni(OH)_2/PtO_2$ interface with one PtO_2 unit on the $Ni(OH)_2$ substrate. To minimize the undesired interactions between images, a vacuum of at least 10 Å was considered along the z axis. The climbing image nudged elastic band (CNEB)[9] method was used to examine the energy profiles along selected pathways for H_2O dissociation.

The ΔG_{H*} was calculated as follows, which is proposed by Norskov and coworkers[10]:

$$\Delta G_{H*} = E_{total} - E_{sur} - E_H^2/2 + \Delta E_{ZPE} - T\Delta S$$

where E_{total} is the total energy for the adsorption state, E_{sur} is the energy of pure surface, E_H^2 is the energy of H_2 in gas phase, ΔE_{ZPE} is the zero-point energy change and ΔS is the entropy change.

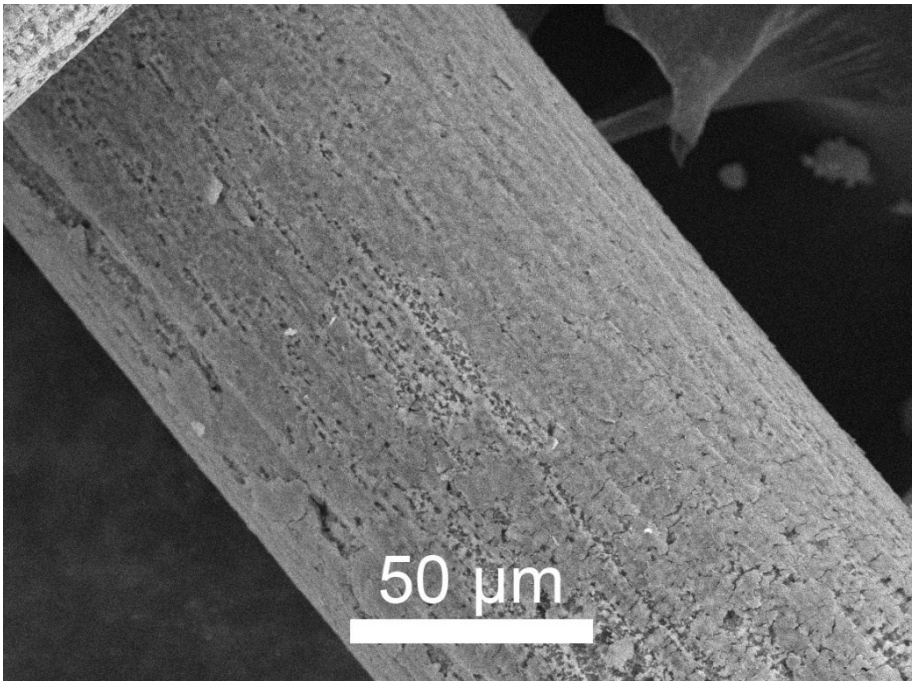

Fig. S1. SEM image of bare Ti mesh.

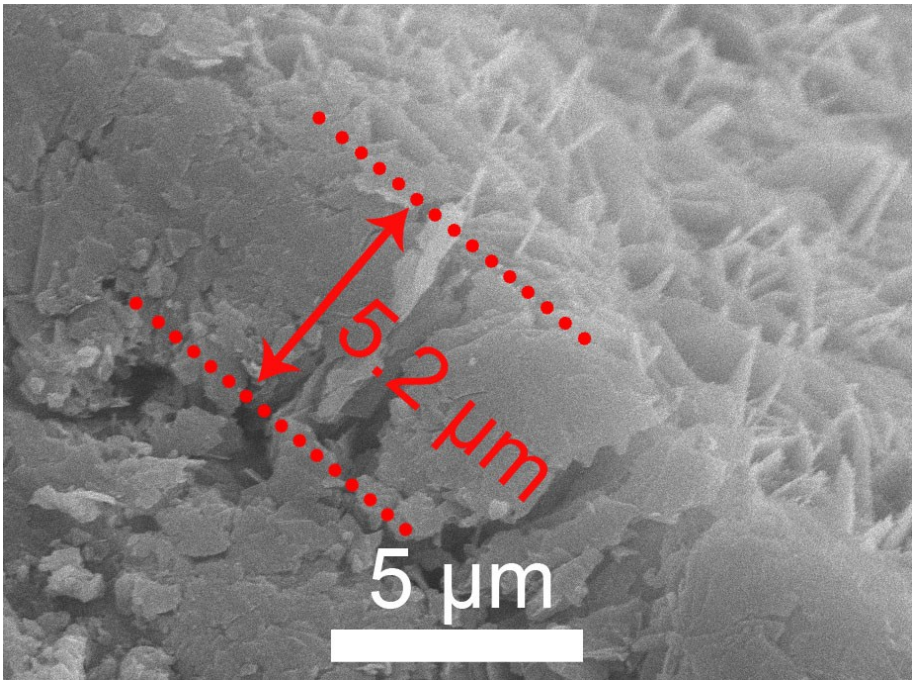

Fig. S2. Cross-section SEM image of $Ni(OH)_2$-PtO_2 NS/Ti.

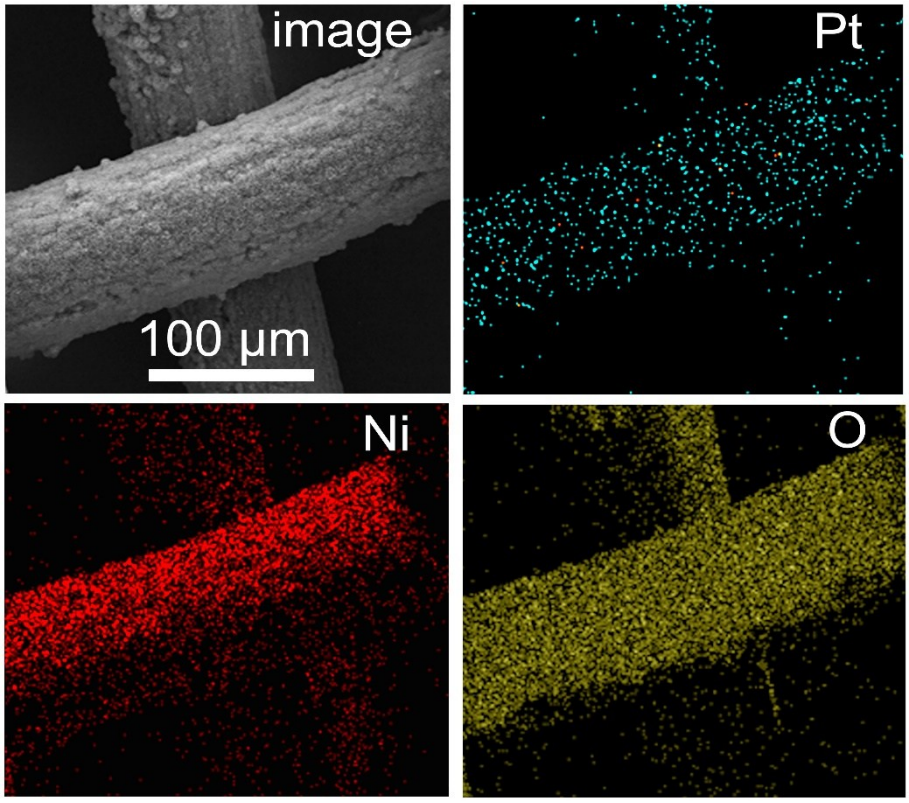

Fig. S3. SEM and EDX elemental mapping images of Pt, Ni and O for $Ni(OH)_2$-PtO_2 NS/Ti.

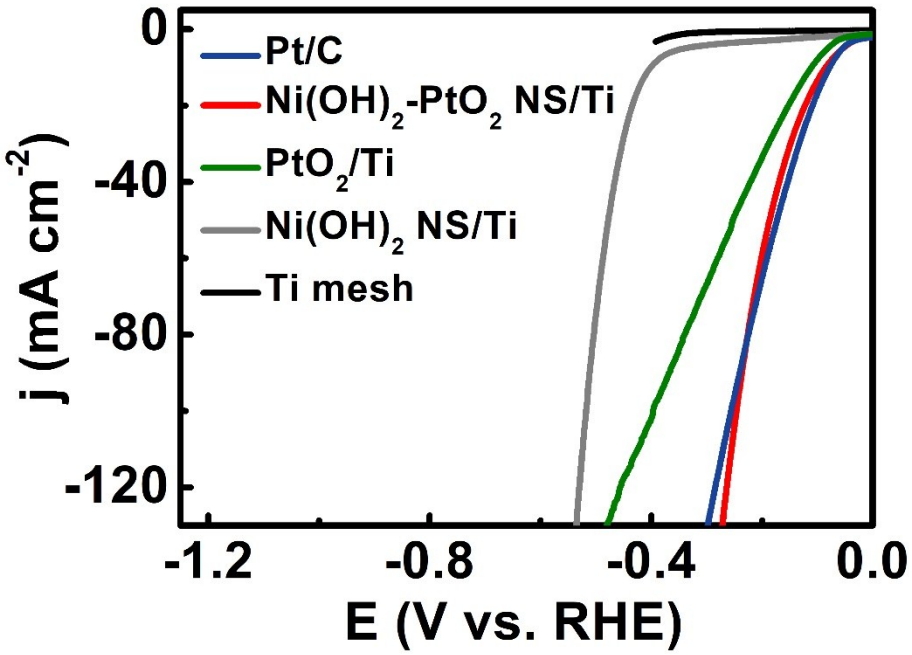

Fig. S4. LSV curves for bare Ti mesh, $Ni(OH)_2$ NS/Ti, $Ni(OH)_2$-PtO_2 NS/Ti, PtO_2/Ti, and Pt/C on Ti mesh with a scan rate of 5 mV s^{-1} for the HER in 1.0 M KOH.

Table S1. Comparison of HER performance for $Ni(OH)_2$-PtO_2 NS/Ti with other Pt-based electrocatalysts in alkaline media.

Catalyst	j ($mA\ cm^{-2}$)	η (mV)	Pt content (wt%)	Electrolyte	Ref.
$Ni(OH)_2$-PtO_2 NS/Ti	4	31.4	5.1	0.1 M KOH	This work
		44.8		1.0 M KOH	
Pt NWs/SL-$Ni(OH)_2$	4	57	38	0.1 M KOH	11
		85		1.0 M KOH	
Pt(110)/$Ni(OH)_2$	4	110	Pt electrode	0.1 M KOH	12
Pt_3Ni frames/$Ni(OH)_2$/C	4	59	20	0.1 M KOH	13
Pt-Ni/C	4	40	25	0.1 M KOH	14
PtCuNi/CNF@CF	4	145	1.8	1.0 M KOH	15
Ni_3N/Pt	4	37	15	1.0 M KOH	16
hcp-Pt-Ni	4	45	39.6	0.1 M KOH	17
Pt_3Ni_2 NWs-S/C	4	60	81.6	0.1 M KOH	18
Pt(111)-$Co(OH)_2$	3	196	Pt electrode	0.1 M KOH/LiOH	19
Pt@2D-$Ni(OH)_2$	4	87	43	0.1 M KOH	20
$Ni(OH)_2$/Pt	5	75	Pt electrode	0.1 KOH	21

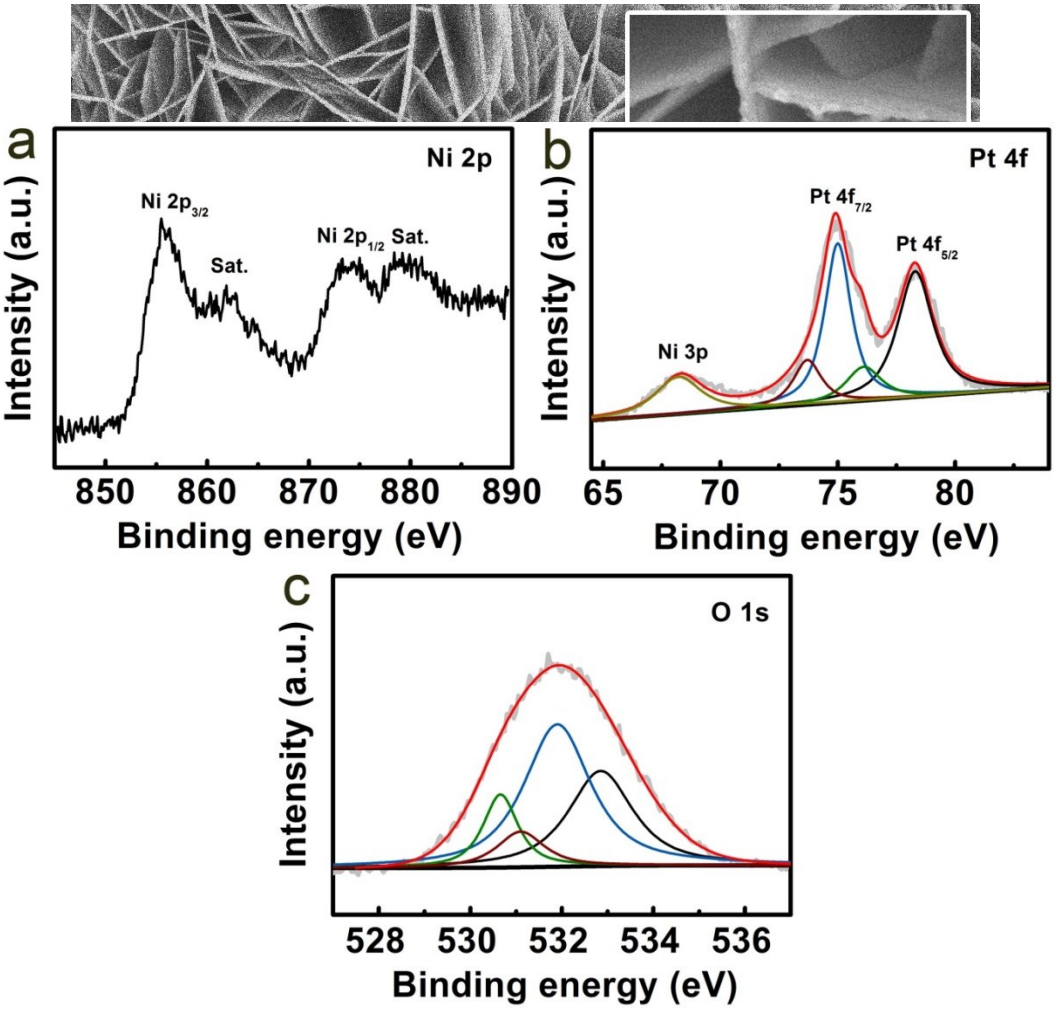

Fig. S5. SEM images of $Ni(OH)_2$-PtO_2 NS/Ti after HER electrolysis in 0.1 M KOH.

Fig. S6. XPS spectra in the (a) Ni 2p, (b) Pt 4f and (c) O 1s regions for $Ni(OH)_2$-PtO_2 after HER electrolysis in 0.1 M KOH.

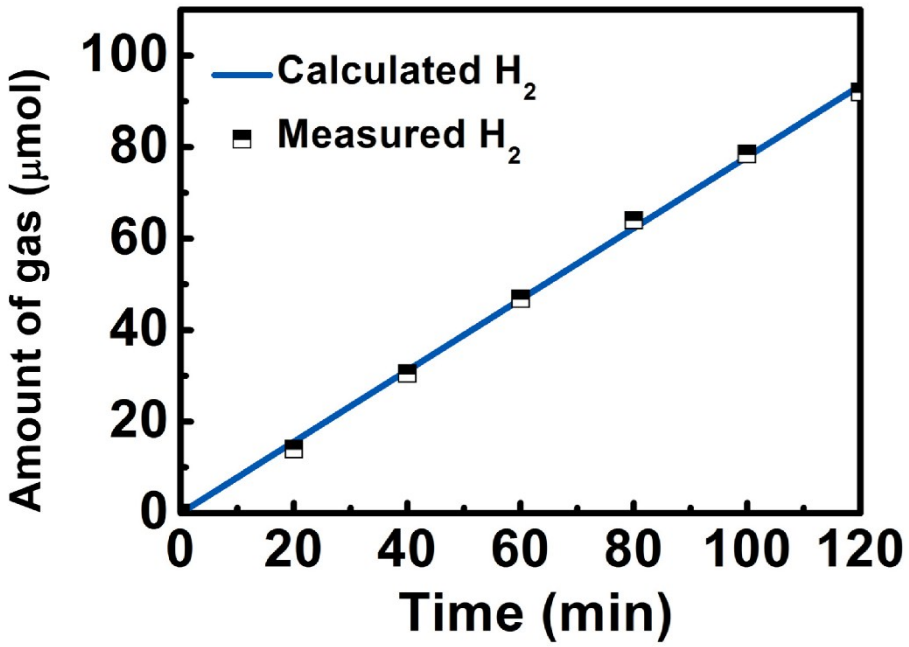

Fig. S7. The amount of gas theoretically calculated and experimentally measured vs. time for $Ni(OH)_2$-PtO_2 NS/Ti in 0.1 M KOH.

References

1 H. Cheng and K. Scott, *J. Appl. Electrochem.*, 2006, **36**, 1361-1366.

2 G. Kresse and J. Furthmuller, *Comp. Mater. Sci.,* 1996, **6**, 15-50.

3 G. Kresse and J. Furthmuller, *Phys. Rev. B,* 1996, **54**, 11169-11186.

4 G. Kresse and J. Hafner, *Phys. Rev. B,* 1994, **49**, 14251-14269.

5 J. P. Perdew, K. Burke and M. Ernzerhof, *Phys. Rev. Lett.*, 1996, **77**, 3865-3868.

6 G. Kresse and D. Joubert, *Phys. Rev. B,* 1999, **59**, 1758-1775.

7 P. E. Blochl, *Phys. Rev. B*, 1994, **50**, 17953-17979.

8 H. J. Monkhorst and J. D. Pack, *Phys. Rev. B*, 1976, **13**, 5188-5192.

9 G. Henkelman, B. P. Uberuaga and H. J. Jónsson, *Chem. Phys.* 2000, **113**, 9901-9904.

10 J. K. Nøskov, T. Bligaard, A. Logadottir, I. R. Kitchin, J. G. Chen, S. Pandelov and U. Stimming, *J. Electrochem. Soc.*, 2005, **152**, J23-J26.

11 H. Yin, S. Zhao, K. Zhao, A. Muqsit, H. Tang, L. Chang, H. Zhao, Y. Gao and Z. Tang, *Nat. Commun.*, 2015, **6**, 6430.

12 R. Subbaraman, D. Tripkovic, D. Strmcnik, K. C. Chang, M. Uchimura, A. P. Paulikas, V. Stamenkovic and N. M. Markovic, *Science*, 2017, **8**, 1256-1260.

13 C. Chen, Y. Kang, Z. Huo, Z. Zhu, W. Huang, H. L. Xin, J. D. Snyder, D. Li, J. A. Herron, M. Mavrikakis, M. Chi. K. L. More, Y. Li, N. M. Markovic, G. A. Somorjai, P. Yang and V. R. Stamekovic, *Science*, 2014, **343**, 1339-1343.

14 R. Kavian, S. I. Choi, J. Park, T. Liu, H. C. Peng, N. Lu, J. Wang, M. J. Kim, Y. Xia and S. W. Lee, *J. Mater. Chem. A*, 2016, **4**, 12392-12397.

15 Y. Shen, A. C. Lua, J. Xi and X. Qiu, *ACS Appl. Mater. Interfaces*, 2016, **8**, 3464-3472.

16 Y. Wang, L. Chen, X. Yu, Y. Wang, and G. Zheng, *Adv. Energy Mater.*, 2017, **7**, 1601390.

17 Z. Cao, Q. Chen, J. Zhang, H. Li, Y. Jiang, S. Shen, G. Fu, B. Lu, Z. Xie and L. Zheng, *Nat. Commun.*, 2017, **8**, 15131.

18 P. Wang, X. Zhang, J. Zhang, S. Wan, S. Guo, G. Lu, J. Yao and X. Huang, *Nat. Commun.*, 2017, **8**, 14580.

19 R. Subbaraman, D. Tripkovic, K.-C. Chang, D. Strmcnik, A. P. Paulikas, P. Hirunsit, M. Chan, J. P. Greeley, V. R. Stamenkovic and N. M. Markovic, *Nat. Mater.*, 2012, **11**, 550-557.

20 L. Wang, Y. Zhu, Z. Zeng, C. Lin, M. Giroux, L. Jiang, Y. Han, J. Greeley, C. Wang and J. Jin, *Nano Energy*, 2017, **31**, 456-461.

21 N. Danilovic, R. Subbaraman, D. Strmcnik, K. C. Chang, A. P. Paulikas, V. R. Stamenkovic and N. M. Markovic, *Angew. Chem.*, *Int. Ed.*, 2012, **51**, 12495-12498.